

Scale-Adv: A Joint Attack on Image-Scaling and Machine Learning Classifiers

Yue Gao
gy@cs.wisc.edu
University of Wisconsin–Madison

Kassem Fawaz
kfawaz@wisc.edu
University of Wisconsin–Madison

Abstract

As real-world images come in varying sizes, the machine learning model is part of a larger system that includes an upstream image scaling algorithm. In this system, the model and the scaling algorithm have become attractive targets for numerous attacks, such as adversarial examples and the recent image-scaling attack. In response to these attacks, researchers have developed defense approaches that are tailored to attacks at each processing stage. As these defenses are developed in isolation, their underlying assumptions become questionable when viewing them from the perspective of an end-to-end machine learning system. In this paper, we investigate whether defenses against scaling attacks and adversarial examples are still robust when an adversary targets the entire machine learning system.

In particular, we propose Scale-Adv, a novel attack framework that jointly targets the image-scaling and classification stages. This framework packs several novel techniques, including novel representations of the scaling defenses. It also defines two integrations that allow for attacking the machine learning system pipeline in the white-box and black-box settings. Based on this framework, we evaluate cutting-edge defenses at each processing stage. For scaling attacks, we show that Scale-Adv can evade four out of five state-of-the-art defenses by incorporating adversarial examples. For classification, we show that Scale-Adv can significantly improve the performance of machine learning attacks by leveraging weaknesses in the scaling algorithm. We empirically observe that Scale-Adv can produce adversarial examples with less perturbation and higher confidence than vanilla black-box and white-box attacks. We further demonstrate the transferability of Scale-Adv on a commercial online API.

1 Introduction

Recent advances in machine learning (ML) techniques have demonstrated human-level performance in many vision tasks, such as image classification [6–8] and object detection [9]. As real-world images come in varying sizes, the ML system includes an image scaling algorithm followed by a downstream ML model. The scaling algorithm resizes input images to match the fixed input size of a model, which takes the input and performs vision tasks, such as classification.

The model and scaling algorithm in an ML system have become attractive targets for attackers. ML models are known as vulnerable to adversarial examples [10, 11]; an adversary can add imperceptible perturbations to the input of a model and change its prediction [4, 5]. Such attacks can take place in the white-box setting where the attacker has access to the model parameters or the black-box setting where the attacker only has access to model outputs or a surrogate model. Recently, scaling algorithms in the ML system were shown as vulnerable to image-scaling attacks [1, 2]; an adversary can manipulate a source image such that it will change into a different target image after scaling, thereby inducing an incorrect prediction in the downstream classifier.

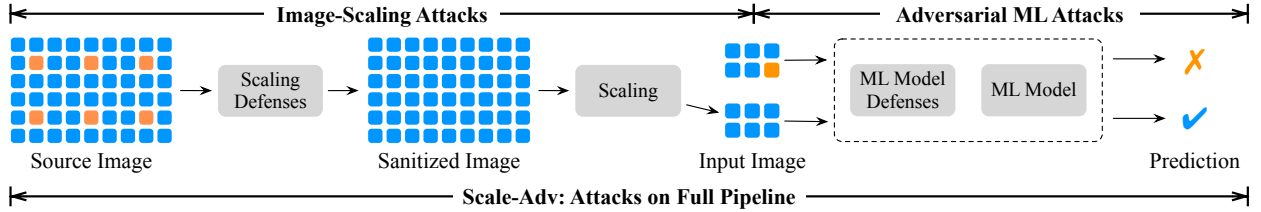


Figure 1: Illustration of the Machine Learning System Pipeline under Different Attacks. The image-scaling attack [1,2] targets the scaling procedure, but it has been shown ineffective under several defenses [2,3]. The adversarial attack [4,5] targets the ML classifier, but there also exist many defenses like adversarial training [5] to mitigate this attack. Our proposed Scale-Adv attack targets the whole ML pipeline. It leverages the benefits of both attacks and poses a critical threat to both defenses.

In response to these attacks, researchers have developed defense approaches tailored to each processing stage. Fig. 1 illustrates an overview of such attacks and defenses in an ML system pipeline. First, several scaling defenses [2, 3] have effectively mitigated the image-scaling attack. These defenses, similar to the scaling attacks, assume the injected target image to be sufficiently different from the source image. Second, robust ML defenses, such as adversarial training [5, 12], defend against adversarial examples of norms below a preconfigured perturbation budget. As these defenses are developed in isolation, their underlying assumptions become questionable when viewing them from the perspective of an ML system.

To attack the ML system, the adversary manipulates an input image to induce a misclassification. The scaling defense, with the underlying assumption of injecting a sufficiently different image, does not fare well if the adversary jointly targets the downstream ML model. For example, the adversary can incorporate adversarial perturbations smaller than the magnitude that the defense was designed to handle. Similarly, the ML defense, which claims robustness against adversarial examples within a certain perturbation budget, can be ineffective if the adversary jointly targets the upstream scaling algorithm. For example, the adversary can leverage weaknesses in image scaling to produce an attack image that satisfies the perturbation budget before scaling, but violates it afterward.

As such, it is necessary to study these attacks and defenses in the context of the ML system pipeline. Such a study informs the effectiveness of cutting-edge defenses for scaling and ML models when the adversary targets the entire ML system. In particular, we are interested in studying the effectiveness of a class of add-on defenses against scaling attacks as well as the robustness properties provided by adversarial training.

This paper proposes Scale-Adv, a new attack framework that jointly targets the image-scaling and classification stages in the ML system. Scale-Adv allows for evaluating defenses against scaling and ML attacks from the perspective of the ML pipeline. Realizing this framework is not straightforward as it requires proper modeling of the scaling defenses and integration with various ML attacks in both white-box and black-box settings. Our attack framework represents scaling defenses as smooth and differentiable functions, which fit as preprocessing steps for arbitrary models. Then, it defines two integrations that allow for attacking the entire ML system pipeline in both white-box and black-box settings.

In the white-box setting, the attack consists of optimizing an objective function that views the ML system pipeline as a sequential model. It generates high-resolution adversarial examples with less perturbation than vanilla attacks on the classifier. While one could question the real-world applicability of the white-box attack, it is useful for two reasons. First, an adversary can deploy this attack on a surrogate model and construct a transfer-based attack against a black-box model. Second, this attack allows for assessing the worst-case robustness of existing scaling defenses through a setting where the attacker has the most

knowledge.

In the black-box setting, the attack consists of a novel hard-label attack that leverages weaknesses in the scaling algorithm to converge faster. This setting is consistent with the scaling attack, which only requires the model to output a label without confidence scores. Our attack evades scaling defenses by jointly targeting the scaling and black-box models. As vanilla black-box attacks are unaware of the weakness in scaling and its defenses, Scale-Adv proposes several techniques to incorporate this knowledge, thus improving their performance.

We integrate our attack framework with cutting-edge ML attacks and scaling defenses after implementing several optimizations to make the attack more effective. We perform our attack in both black-box and white-box settings and compare our performance against the powerful attacks we integrate. Our evaluation reveals three main findings:

- In both the black-box and white-box setting, we show that Scale-Adv can evade four out of five state-of-the-art scaling defenses. These defenses include the median filtering by Quiring et al. [2] and all three detection defenses by Kim et al. [3]. However, we find that randomized filtering by Quiring et al. is robust to our attack even in the white-box setting. Further, we provide a theoretical argument to explain the robustness properties of these defenses.
- In the black-box setting, Scale-Adv successfully leverages the weakness in scaling algorithms (even under defenses) to improve the performance of black-box attacks by a large margin. For the same query budget, Scale-Adv is able to generate less perturbed adversarial examples than vanilla black-box attacks such as HopSkipJump [13].
- Finally, we show that Scale-Adv can significantly improve cutting-edge ML attacks in the white-box setting. For the same perturbation budget, it generates stronger and more confident adversarial examples than vanilla white-box attacks such as PGD [5] and C&W [4]. We further show how Scale-Adv can attack a surrogate model to generate less perturbed adversarial examples that transfer to a commercial online API.

2 Background

In this section, we briefly review the background necessary to understand the ML system pipeline, as well as the attacks and defenses for image-scaling and ML models.

2.1 Machine Learning System Pipeline and Image Scaling

ML models designed for vision tasks accept image inputs of a fixed size. For example, the widely used model ResNet [14] accepts 224×224 input images¹. As real-world images come in varying sizes, the ML model is part of a larger ML system that includes image scaling, as illustrated in Fig. 1. The end-to-end ML pipeline accepts an input image S in high resolution. It includes a scaling stage that downscales S to D in low-resolution, which matches the input dimensions of the ML model. The ML model takes image D as an input and predicts a corresponding label; we mainly focus on downstream models that perform classification. As the background for ML models is well-documented in the literature, we focus on the less-explored scaling procedure in the remainder of this section.

¹We will omit the channel dimension in the rest of this paper.

The scaling procedure, $\text{scale}(\cdot)$, resizes a high-resolution (HR) source image $S \in \mathbb{R}^{m \times n}$ to the low-resolution (LR) output image $D \in \mathbb{R}^{p \times q}$. In this procedure, we define the overall scaling ratios as $\beta = \min\{\beta_h, \beta_v\}$, where $\beta_h = n/q$ and $\beta_v = m/p$ are the scaling ratios in two dimensions. In this paper, we only consider downscaling where $\beta > 1$.

The scaling function can be implemented in different ways, but researchers have identified two unified formulations of this function: matrix multiplication and convolution.

2.1.1 Matrix Multiplication

Xiao et al. [1] conduct the first empirical analysis of the common scaling function. They represent image scaling as matrix multiplications:

$$D = \text{scale}(S) = L \times S \times R, \quad (1)$$

where $L \in \mathbb{R}^{p \times m}$ and $R \in \mathbb{R}^{n \times q}$ are the two constant coefficient matrices determined by the applied scaling function. They also propose an efficient strategy to extract approximations of these matrices from given implementations.

2.1.2 Convolution

Quiring et al. [2] interpret scaling as a convolution between the source image S and a fixed linear kernel k determined by the scaling algorithm². They represent the scaling function as:

$$D = \text{scale}(S) = S \star k, \quad (2)$$

where \star denotes the 2D convolution with proper padding and stride size to match the desired output shape.

2.2 Image-Scaling Attacks

The scaling attack targets the scaling procedure in an ML system pipeline. Xiao et al. [1] and Quiring et al. [2] have demonstrated that an attacker can exploit the scaling procedure to compromise an arbitrary downstream ML model. Fig. 2 illustrates the pipeline of this attack. An adversary computes the attack image A by adding imperceptible perturbations Δ to the source image S , such that it will become similar to a target image T (with a different label from S) after scaling, thereby inducing an incorrect prediction on the downstream classifier. Based on the above pipeline, they formulate the scaling attack as a quadratic optimization problem:

$$\min \|\Delta\|_2^2 \quad \text{s.t.} \quad \|\text{scale}(S + \Delta) - T\|_\infty \leq \epsilon, \quad (3)$$

where the attack image $A \triangleq S + \Delta$ should also satisfy the box constraint $A \in [0, 1]^{m \times n}$. They solve this problem using Quadratic Programming. Later, Chen et al. [16] formulated it as an unconstrained problem that can be solved efficiently using gradient-descent minimization techniques.

In addition to the above empirical attacks, Quiring et al. [2] conducted an in-depth analysis of common scaling algorithms and corresponding convolution kernels used in Eq. (2). They identified the non-uniform kernels of a fixed-width during the scaling procedure as the root cause of scaling attacks. Such kernels assign higher weights to a small set of *vulnerable pixels* in the source image. For example, in Fig. 2, the attacker only needs to modify a few vulnerable pixels (orange) in the attack image to change the scaling output completely.

²Precisely, this is a cross-correlation. But we will use the term convolution for simplicity and to stay consistent with most of the ML literature [15].

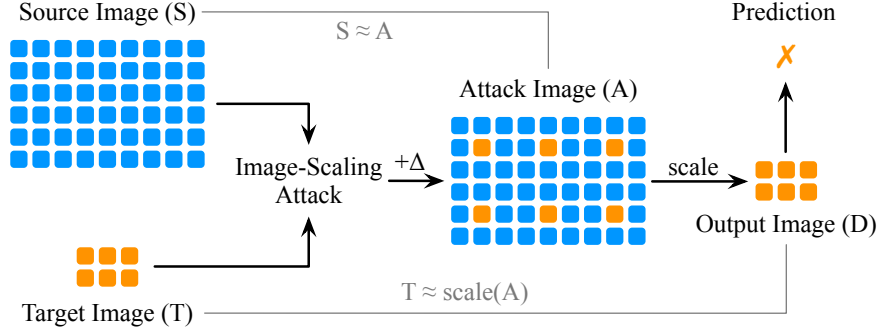


Figure 2: Image-Scaling Attack Pipeline. The adversary computes the attack image A such that it looks similar to the source image S , but will downscale to the target image T .

The scaling attack does not require knowledge of model parameters. Instead, it only needs hundreds of black-box queries to infer the scaling algorithm in an ML system [1].

2.3 Image-Scaling Defenses

Researchers have proposed several add-on defenses against the scaling attack; these defenses fall into two categories: prevention and detection defenses. Below, we review five state-of-the-art defenses that work for all scaling attacks. We summarize their techniques in Tab. 1.

2.3.1 Prevention Defenses

Quiring et al. [2] propose the only two prevention defenses, i.e., median and randomized filtering. Both defenses apply filtering operations to sanitize the input image before scaling. Specifically, they reconstruct each vulnerable pixel by the median or randomly picked pixel within a sliding window. As a result, an adaptive attacker has to perturb a significantly larger number of pixels within a window to evade these defenses. Quiring et al. claim that the median filtering defense is more practical; the randomized filtering defense could hurt the downstream classifier’s performance [2], which requires model retraining.

2.3.2 Detection Defenses

Kim et al. [3] propose the most effective detection defenses. They present three detection methods using spatial and frequency transformations: unscaling, minimum-filtering, and centered spectrum. These trans-

Table 1: Summary of the technique used by recent scaling defenses.

Defense	Type	Technique
Median [2]	Prevention	Apply median filtering in a window.
Randomized [2]	Prevention	Randomly sample pixels in a window.
Unscaling [3]	Detection	Apply down- and up-scaling to detect perturbation.
Min-filtering [3]	Detection	Apply min-filtering to reveal injected perturbation.
Spectrum [3]	Detection	Identify peaks in the centered spectrum.

formations result in discernible differences when being applied to benign and attack images. The unscaling invokes downscale and upscale operations sequentially to reveal the injected image. If the input image is benign, this procedure should reveal a similar image to the input. In the case of an attack image, this sequence would reveal a different image. Similarly, minimum-filtering reveals such differences using the minimum filter operation. By measuring this difference, they construct a threshold-based detector using mean squared error (MSE) and structural similarity index (SSIM). Similarly, the attack perturbation manifests as high-energy and high-frequency noise, which is detectable from the centered spectrum.

2.3.3 Robust Scaling Algorithms

Quiring et al. [2] have identified several scaling algorithms that are naturally robust to the scaling attack. These algorithms are robust because they use either uniform kernels or dynamic kernel widths. For instance, the area scaling algorithm convolves the input image (of scaling ratio β) with a uniform kernel κ_{area} of size $\beta \times \beta$, where each entry of κ_{area} is set to $1/\beta^2$ – the kernel considers each pixel in the window equally.

Ideally, such algorithms should be part of the ML pipeline, but add-on defenses protecting non-robust scaling algorithms are considered more practical. As the default scaling algorithm in common ML frameworks is not robust [2], switching to a different (robust) scaling algorithm faces compatibility issues, such as changing dependent libraries, performance degradation, and even model retraining. As such, deployed ML systems would prefer add-on defenses that can easily fit as plugin modules [3].

In this paper, we show that add-on defenses are not robust against the adversary that targets the whole ML system pipeline. We further show that the adversary can leverage weaknesses in these algorithms to mount stronger black-box and white-box attacks. Based on our results, we conclude that ML systems need to avoid such add-on defenses; they should deploy scaling algorithms that are robust by design.

2.4 ML Model Attacks

The ML models in the pipeline are vulnerable to ML attacks. In this paper, we consider untargeted evasion attacks that aim to induce a misclassification with minimum ℓ_2 -norm perturbation to an input. Such attacks can take place in different threat models, such as white-box and black-box.

2.4.1 White-box Attacks

Most attacks have studied the white-box setting, where the attacker has full knowledge of the model parameters. In this case, the main objective is to minimize the adversarial perturbation. Examples of powerful white-box attacks include C&W [4] and PGD [5].

The C&W [4] attack solves the following optimization problem to find the minimal adversarial perturbation δ for an input image x :

$$\min_{\delta} \|\delta\|_2 + c \cdot f(x + \delta) \quad \text{s.t. } x + \delta \in [0, 1]^n, \quad (4)$$

where c is a constant determined by a binary search procedure and f is a loss function quantifying the confidence of ground-truth prediction. While we do not expand f here, we note that the confidence is controlled by a parameter κ . An attacker can increase κ to produce more confident adversarial examples.

The PGD [5] attack employs an iterative algorithm to solve the following constrained optimization problem:

$$\max_{\delta} J(\text{model}(x + \delta), y) \quad \text{s.t. } \|\delta\|_2 \leq \epsilon, \quad (5)$$

where ϵ upper-bounds the adversarial perturbation in ℓ_2 -norm space, y is the ground truth label, and J is the cross entropy loss. This attack can be used to assess the model’s robustness against an attacker given certain perturbation budget.

2.4.2 Black-box Attacks

In this setting, the attacker does not have knowledge of the model parameters. But, the attacker can send hard-label (decision) or soft-label (prediction score) queries to the model. As queries come with monetary costs, the main objective is to minimize the perturbation as well as the number of queries. For the purpose of this paper, we only consider the more challenging hard-label setting.

Most hard-label attacks choose to walk near the decision boundary, such as the recent HopSkipJump [13] attack. These attacks employ an iterative algorithm to solve the following optimization problem:

$$\min_{x'} \|x' - x\|_2 \quad \text{s.t. } x' \text{ is misclassified.} \quad (6)$$

The iterative algorithm can be summarized in three steps: (1) Find a point x' near the decision boundary through a linear search; (2) Sample noise around x' to estimate the gradient; (3) Use the gradient to update x' . This algorithm usually finds an adversarial example at the beginning but requires more iterations to decrease the perturbation size.

2.5 ML Model Defenses

Researchers have implemented numerous defenses to mitigate evasion attacks against the classifier. In this paper, we consider adversarial training [5], which is one of the most effective empirical defenses [12]. It views adversarial examples (produced by the white-box attack discussed above) as the worst-case examples and includes them in the training data. It serves as a strong baseline to assess evasion attacks.

3 Scaling Defense Analysis

Existing scaling attacks, thus far, have only considered feeding the classifier a clean image (without adversarial perturbation) to change its prediction; we refer to this as the “clean-image” assumption. This approach is beneficial because it allows attacking an arbitrary downstream model. The problem with this approach, however, is that state-of-the-art defenses are also tailored to the same assumption. This assumption becomes questionable when viewing it from the perspective of the entire ML system; all ML models for vision tasks are preceded by a scaling stage. For example, an attacker can circumvent this assumption by incorporating adversarial perturbations. It is not clear if existing defenses are still effective in this case. As such, there is a need to re-study these defenses without the clean-image assumption.

In this section, we provide a theoretical intuition to study the robustness of add-on scaling defenses. We find their robustness relies on the assumption that injected perturbations manifest as high-frequency and high-energy noise. This assumption does not hold if the adversary injects adversarial perturbations.

3.1 Robust Prevention Defenses

Quiring et al. [2] observe that a robust scaling algorithm should uniformly weight all the pixels in an input image. However, they have not made a similar argument for the prevention defenses they propose. To complement their theoretical arguments, we note that any argument about the robustness requirement for a

scaling algorithm should apply to the defense approach as well. In particular, we can represent the defended scaling function as a composition: $\text{scale} \circ \text{defense}$. Since we can view this composition as a new scaling function, it must also satisfy the requirement of uniform weighting to be robust. This simple observation indicates that an effective defense should process the input such that any non-robust scaling function will uniformly weight all pixels.

3.2 Median Filtering

The median filtering defense sanitizes the input image by sliding a window w around vulnerable pixels and applying the median filter f_{med} . To evade this defense, an adaptive attacker may perturb pixels in each window w , such that the filtering output $w_m = f_{\text{med}}(w)$ changes to the desired value w_t [2].

Although Quiring et al. [2] consider the median filtering as a robust defense, we note that this defense fails to satisfy their robustness requirement of uniform weighting. An adaptive attacker only needs to set pixels within a particular range $R \triangleq [w_m, w_t]$ to w_t to change the filter’s output [2]. Since $|R| \leq |w|/2$, the attacker needs only modify at most half of the pixels to change the filtering output into a target value. Thus, this defense cannot provide a uniform weight for at least half of the pixels in w .

We find it possible to evade this defense from the above observation. The median filtering defense’s robustness heavily relies on the value of $|R|$, which is large only if the injected perturbation manifests as high-frequency and high-energy noise (resulting from the clean-image assumption). Injecting low-energy noise such as adversarial perturbations could potentially compromise the defense’s effectiveness for two reasons. First, an adversarial example typically has smaller distortions to the scaled source image, so the target pixel w_t is closer to the original pixel w_m , implying a smaller range $R = [w_m, w_t]$ than injecting a completely different image. Second, the classifier returns the same prediction even if the target pixel is not matched precisely where $f_{\text{med}}(w) = w_t - \epsilon$ for a small constant ϵ . Since the value of ϵ is indefinite, a smarter adaptive attacker can optimize ϵ jointly for all windows, thereby also decreasing the perturbation.

Given the above arguments, we find that the median filtering defense is most effective against high-frequency and high-energy noise. However, it is not designed to handle low-energy noise, such as the injected adversarial perturbation.

3.3 Randomized Filtering

The randomized filtering defense sanitizes the input image by sliding a window w around vulnerable pixels and applies the random filter f_{rnd} , which randomly picks a pixel from w . To evade this defense completely, an adaptive attacker has to set every pixel in the window w to the desired value [2].

We find that the randomized filtering defense can process the input such that any scaling function will give a uniform weight to all pixels in expectation, meeting the robustness requirement. We provide a theoretical argument in Appendix A to show that the expectation of randomized filtering defense can be described as

$$\mathbb{E}_{\text{defense} \sim \mathcal{D}}[(\text{scale} \circ \text{defense})(S)] = S \star k_{\text{area}}, \quad (7)$$

where \mathcal{D} is the space of defense functions chosen by the randomized filtering defense and k_{area} is the uniform area scaling kernel defined in Sec.2.3.3.

Therefore, we expect this defense to handle any kind of noise, including the injected adversarial perturbation.

3.4 Detection Defenses

Detection defenses aim to detect the perturbations injected by scaling attacks. A detector determines whether the input image $x \in \{S, A\}$ is benign (S) or perturbed by the scaling attack ($A = S + \Delta$). In this section, we study the detection defenses from Kim et al. [3], as summarized in Tab. 1.

In the spatial domain, both the unscaling and min-filtering methods reveal the injected perturbation through processing the input image x with some function h . Once revealed, they quantify the resulting distortion with perceptual metrics like MSE and SSIM. For instance, one could examine the distortion score by $t(x) \triangleq \text{MSE}(x - h(x))$. Then, a threshold-based detector examines $t(x)$ and determines whether x is benign or perturbed.

In the frequency domain, center-spectrum defense examines peaks in the spectrum image, as injected perturbations manifest as high-frequency and high-energy noise. Specifically, it applies a low-pass filter on the input’s spectrum image. Although this defense examines the perturbation in the frequency domain, the applied low-pass filter still relies on a threshold.

The above detection defenses all rely on a threshold-based mechanism. This threshold, however, is only easy to find under the clean-image assumption. Once this assumption does not hold, there may not exist a threshold to allow for acceptable false acceptance and rejection rates. For example, suppose the distortion score t on benign images is typically smaller than a threshold t^* . Then, it suffices to upper bound the perturbation by t^* to evade such detectors.

Given the above arguments, we find that existing detection defenses are most effective against high-energy noise (like the median filtering defense discussed above). Such defenses are not designed to handle low-energy noise, such as the injected adversarial perturbation.

4 Scale-Adv Attack Framework

The prevention and detection defenses effectively block the existing scaling attacks. Our analysis in Sec. 3, however, shows that almost all existing defenses fall under the clean-image assumption. Thus, there is a need to re-study existing scaling defenses without this assumption.

Similar to scaling defenses that have been developed in isolation of the ML model, current ML defenses are developed in isolation from the scaling algorithm. These ML defenses can be ineffective if the adversary jointly targets the upstream scaling algorithm. For example, adversarial training provides empirical robustness against adversarial perturbation within certain ℓ_p -norm budgets. The adversary can leverage scaling attack to obtain an attack image that satisfies the perturbation budget before scaling but violates this budget after scaling. Thus, there is also a need to examine ML defenses in the context of the whole ML system.

To this end, we propose Scale-Adv, a new attack framework that jointly targets the scaling and the classifier in the black-box and white-box settings. Scale-Adv explicitly incorporates scaling, scaling defenses, and classification stages in the attack loop. This design leverages the benefits of both scaling attacks and existing attacks on the classifier.

In the remainder of this section, we discuss our threat model and present the pipeline of our attack framework. Then, we explain how to model scaling defenses for the purpose of our attack.

4.1 Threat Models

We consider both *black-box* and *white-box* settings. In the black-box setting, the attacker has no knowledge of the model parameters. The attacker can only send hard-label queries to the ML system. It only observes the final decision or the predicted label. To stay consistent with previous work studying black-box attacks,

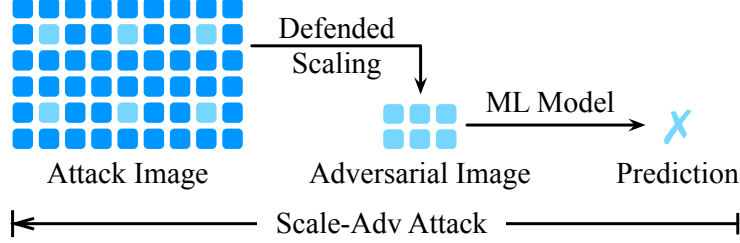


Figure 3: Illustration of the Scale-Adv Attack Pipeline.

the victim ML model does not deploy any defenses, such as adversarial training. Alternatively, the attacker can employ transfer-based attacks by running white-box attacks on a surrogate model.

In the white-box setting, the attacker has complete knowledge of the model parameters. To provide a fair threat model, we protect the victim ML model with adversarial training so that it is empirically robust to certain attacks. Otherwise, it would be straightforward to compromise the naturally trained model and generate imperceptible perturbations.

In both settings, we assume the knowledge of deployed scaling algorithms and defenses. This assumption is reasonable because such settings can be easily inferred [1]. As there are only limited types of scaling defense, the attacker can also infer this knowledge by enumerating all the defenses.

4.2 Attack Pipeline

Scale-Adv incorporates the scaling algorithm, scaling defenses, and classifier in the attack loop, as illustrated in Fig. 3. We instantiate the Scale-Adv attack by two steps: (1) represent the scaling algorithm, scaling defenses, and classifier as a sequential model, and (2) deploy a chosen ML attack on this model. The attack can take place in both white-box and black-box settings.

However, realizing this framework is challenging. First, all existing scaling defenses lack a differentiable formulation that can be successfully leveraged for a white-box attack. It is not straightforward to represent the entire pipeline as a sequential model. Second, naively deploying a black-box attack on this sequential model is ineffective, as it is unaware of the weakness in scaling. The vanilla black-box attack does not exploit the scaling algorithm even if it targets the entire ML system pipeline.

To address the above two challenges, we first model existing scaling defenses as differentiable functions. This allows us to represent the entire ML system pipeline as a sequential model, which enables effective white-box attacks. We also propose several optimizations, such as cached sampling, to make the attack more efficient (Sec. 5). For black-box attacks, we look into the original attack’s algorithm to incorporate the knowledge of scaling algorithms and defenses. This improvement allows black-box attacks to target the entire ML system, and more importantly, leverage the weakness in scaling algorithms (Sec. 6).

4.3 Model Prevention Defenses

As evading the prevention defenses is a core component in Scale-Adv, we will first explain how to model filtering-based prevention defenses.

4.3.1 Masked Pooling Layer

Since prevention defenses perform a filtering operation over the vulnerable pixels, we model them as a masked pooling layer. For simplicity, we describe the pooling layer as a convolution, because the pooling layer works like a discrete convolution but replaces the linear kernel with some other function [17]. Thus, we represent the defense as

$$\text{defense}(x) \triangleq p(x) \cdot \text{mask} + x \cdot (1 - \text{mask}), \quad (8)$$

where p is the pooling function, mask is a boolean mask with 1 denoting vulnerable pixels. The pooling function is given as: $p(x) \triangleq x \star f$, where \star denotes the 2D convolution with reflect padding to keep the same shape, and f denotes the filter function determined by the defense.

4.3.2 Vulnerable Pixels Identification

We propose a simple strategy to determine the boolean mask in Eq. (8). For any fixed scaling algorithm (with input shape $m \times n$ and output shape $p \times q$), we can write the scaling function as a matrix multiplication like Eq. (1). By setting all entries in the output image $D \in \mathbb{R}^{p \times q}$ to 1 and solving for S , we have

$$S^* = L^+ \times D \times R^+ \in \mathbb{R}^{m \times n}, \quad (9)$$

where L^+ and R^+ are the pseudo-inverse [18] of L and R . Conceptually, this recovers the element-wise weight of each pixel in the source image during scaling. As such, every non-zero entry in S^* indicates a vulnerable pixel in the source image S ; we finally determine the mask in Eq. (8) as

$$\text{mask} = \mathbb{1}\{S \neq 0\}, \quad (10)$$

where the indicator function $\mathbb{1}$ and operator \neq are all computed in element-wise.

4.4 Integration with Different Attacks

The above formulation provides the basic intuition of how to model prevention defenses in our attack framework. In the rest of this paper, we provide the integration of scaling defenses with powerful white-box and black-box attacks.

We integrate white-box attacks in Sec.5. Extending from the above formulation, we also explain how to incorporate the randomized filtering defense and detection defenses. The chosen white-box attacks include C&W [4] and PGD [5].

We integrate black-box attacks in Sec.6. This integration is more challenging and requires several key insights of the original attack. In this case, we do not model detection defenses, as we empirically find that the proposed attack naturally evades such defenses without attacking them explicitly. We also skip the randomized filtering, as we empirically observe that such defense is robust even in the white-box setting.

5 Integration with White-box Attacks

In this section, we explain how to integrate Scale-Adv with white-box attacks such as C&W [4] and PGD [5]. We also explain how to incorporate the randomized filtering defense and detection defenses in the attack loop. Further, we propose a technique called cached sampling to make the attack on randomized filtering more efficient.

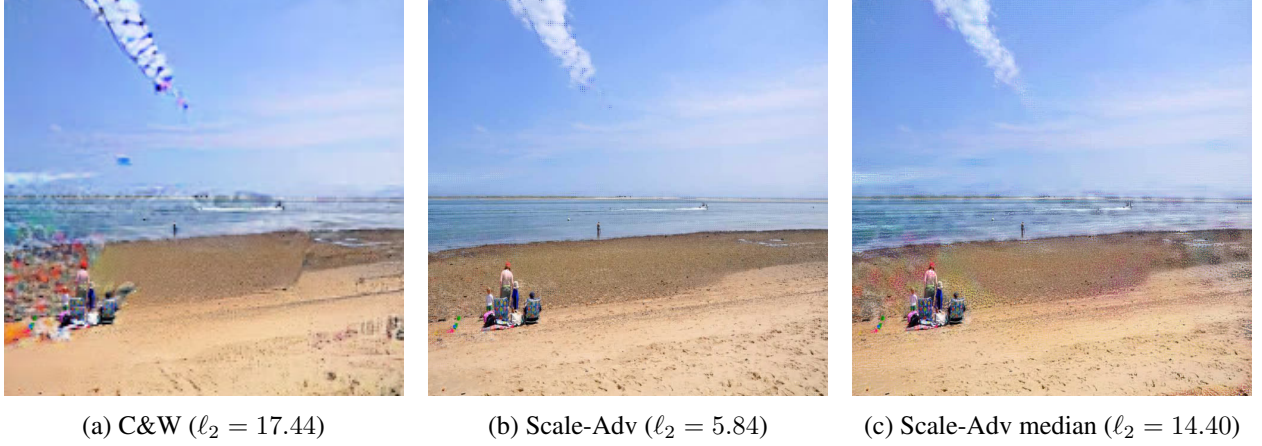


Figure 4: Adversarial examples from (a) C&W attack, (b) Scale-Adv attack, and (c) Scale-Adv attack under median filtering defense. The confidence parameter is set to $\kappa = 2$. The original shape is 224×224 for (a), and 672×672 for (b) and (c). This shows that Scale-Adv can produce less perturbation than C&W attack even under the median filtering defense.

5.1 White-box Attacks

In the white-box setting, the attacker has complete knowledge of the model parameters. Since we have formalized the scaling algorithm and prevention defenses as differentiable functions, we can view the whole ML pipeline as a sequential model and directly deploy existing attacks.

For C&W attack [4], our objective function is

$$\begin{aligned} \min \quad & \|\Delta\|_2 + c \cdot (f \circ \text{scale} \circ \text{defense})(S + \Delta) \\ \text{s.t.} \quad & S + \Delta \in [0, 1]^n, \end{aligned} \quad (11)$$

where f is the loss function quantifying the confidence of ground-truth prediction, S is the HR source image, and Δ is the HR adversarial perturbation.

For PGD attack [5], our objective function is

$$\begin{aligned} \max \quad & J((\text{model} \circ \text{scale} \circ \text{defense})(S + \Delta), y) \\ \text{s.t.} \quad & \|\Delta\|_2 \leq \epsilon, \end{aligned} \quad (12)$$

where $J(\cdot)$ is the cross entropy loss, y is the ground truth label of S , and ϵ is the specified perturbation budget.

5.2 Attack Median Filtering

We find the gradient of median filtering to be useful in the white-box setting. In this case, we instantiate the defense function in Eq. (8) with the pooling function $p(x) = x \star f_{\text{med}}$, where f_{med} is the median filter. Fig. 4 shows the adversarial examples produced by our Scale-Adv attack when integrating with the C&W attack of $\kappa = 2$. This figure highlights the effectiveness of our attack against median filtering.

5.3 Attack Randomized Filtering

As randomized filtering returns random outputs, we apply Expectation over Transformation [19] to correctly compute the gradient over the expected filtering operation.

We have modeled prevention defenses in Eq. (8) as a masked pooling layer with some fixed pooling function p . To model randomness, the pooling function p can be viewed as a random variable drawn from \mathcal{P} , the space of pooling functions that map input images to any images generated by the randomized pooling. We adopt Monte Carlo sampling to approximate the expectation of the defense function in Eq. (8), written as

$$\mathbb{E}[\text{defense}(x)] = \frac{1}{N} \sum_{p_i \sim \mathcal{P}, i \in [N]} p_i(x) \cdot \text{mask} + x \cdot (1 - \text{mask}), \quad (13)$$

where N is the number of samples in Monte Carlo sampling. The choice of N depends on the number of pixels within a sliding window. We empirically set $N = 20$ as the filtering considers 5×5 sliding windows. Thus, our attack integrates the randomized filtering defense by replacing the defense function in Eqs. (11) and (12) with its expectation from Eq. (13).

In practice, however, we find this attack inefficient due to a large number of sampling operations. For example, the adversary needs to recompute Eq. (13) in every iteration. As the input x is unlikely to change significantly in a few iterations if given a reasonable learning rate, we notice that the corresponding output would also not change by a large margin. Based on this observation, we propose a new technique, cached sampling, to make the attack more efficient.

We begin with an empirical study of the sampling’s output. We sample the element-wise distortion (over vulnerable pixels) between a fixed input x and its randomized filtering output $\text{defense}(x)$. We are able to observe that the distortion follows a Laplacian distribution (examples shown in Appendix D). Given this zero-concentrated distribution, we propose to approximate such a distribution by relaxing its dependence on the input x , and reuse the same distortion within a small range of iterations. To this end, we model the output as a fixed concentration μ_x (depending on the input x) with additive noise η , where we can cache the sampled noise as

$$\{\eta_i\}_{i=1}^N \stackrel{\text{iid}}{\sim} \text{defense}(x) - x. \quad (14)$$

We rewrite the defense function (at the k -th iteration) as

$$\text{defense}(x_{k+1}) \triangleq \mu_{x_k} + \eta, \quad (15)$$

where we only resample the noise η for every τ iterations, reducing the number of samples by a constant factor of τ . We empirically set $\tau = 20$. A larger value of τ could cause the attack unable to find an effective attack image.

Note that our analysis in Sec. 3.3 shows that the randomized filtering defense is, in expectation, equivalent to the area scaling. In this case, μ_x is given as $\mu_x = x \star k_{\text{area}}$, where k_{area} is the area scaling kernel. The random filtering can thus be viewed as an average pooling layer.

5.4 Attack Detection Defenses

We empirically observe that Scale-Adv can evade all state-of-the-art detection defenses without explicitly attacking them. Despite that, we provide a generic methodology to instantiate effective adaptive attacks against detection defenses.

We represent the attack from Carlini et al. [20] against a learning-based detector [21]. Given any detection function g , we follow their two-step process. First, we choose a loss function L so that $L(S + \Delta)$ is

minimized when the detection $g(S + \Delta)$ is incorrect. Second, we add the loss function L as a regularizer to our objective functions in Eqs. (11) and (12). For instance, Eq. (12) would become

$$\begin{aligned} \max J((\text{model} \circ \text{scale} \circ \text{defense})(S + \Delta), y) - \gamma \cdot L(S + \Delta) \\ \text{s.t. } \|\Delta\|_2 \leq \epsilon, \end{aligned}$$

where γ is the hyper-parameter that controls the weight of added regularizer.

6 Integration with Black-box Attacks

In this section, we explain how to integrate Scale-Adv with black-box attacks. In particular, we integrate with the recently proposed hard-label attack HopSkipJump [13].

6.1 Black-box Attacks

In the hard-label setting, the attacker can only send queries to acquire the hard-label decision instead of the probability or confidence score. As such, most attacks choose to walk near the decision boundary while minimizing the perturbation size. HopSkipJump [13] is one of such powerful attacks.

Although such attacks can be deployed to any black-box system, including the complete ML pipeline that accepts HR input images, we note that blindly attacking the entire pipeline cannot leverage the benefits of scaling attacks. In other words, vanilla HopSkipJump attack cannot benefit from attacking the whole ML system with HR input images.

To address this challenge, we modify the iterative algorithm (see Sec.2.4.2) in this attack to incorporate the knowledge of upstream scaling algorithms. In particular, we incorporate this knowledge in the noise sampling procedure, which is used to estimate the gradient information. As such, our Scale-Adv attack can be summarized in three steps: (1) Find a point x' near the decision boundary through a line search from the input x along a given direction; (2) Sample noise around x' that *incorporates the knowledge of scaling* to estimate the gradient at the decision boundary; (3) Use the gradient to update the direction to search for a new x' .

We develop several techniques to incorporate the knowledge of scaling (Sec.6.2) and the median filtering defense (Sec.6.3). Fig.6 shows the adversarial examples produced by the Scale-Adv attack with a 5K query budget. We provide more examples in AppendixE. Our attack is able to obtain less perturbation than vanilla HopSkipJump.

6.2 Attack Scaling

To incorporate the knowledge of scaling, we first note that most scaling algorithms can be viewed as a linear mapping from the high-resolution (HR) space to a low-resolution (LR) subspace embedded within the HR space. A vanilla attacker (without leveraging the scaling) estimates the gradient using noise sampled in the HR space, which is suboptimal. Scale-Adv incorporates the knowledge of the scaling procedure by constraining sampled noise in the LR subspace. It samples noise in the HR space that lies on the LR subspace.

We propose a simple two-step procedure to sample noise that lies on the LR subspace: (1) sample noise u' in the LR subspace; and (2) project the LR noise u' back to the HR space. Fig.5 illustrates this new sampling procedure. The first step is straightforward as the LR subspace is well-defined by the scaling

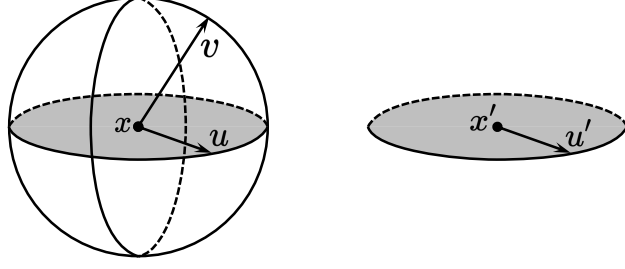


Figure 5: Illustration of noise sampling. In the HR space (left), commonly sampled noise v is unlikely to find the exploitable subspace. We instead sample noise u' in the LR space (right), and project it back to u , which lies on the LR subspace.

algorithm. In the second step, a straightforward solution is to compute the exact projection by solving an optimization problem as

$$\min_u \|\text{scale}(x + u) - (\text{scale}(x) + u')\|_2, \quad (16)$$

where u is the HR noise.

However, this approach incurs computational overheads, as we need to solve an optimization problem for *every* noise sample. To overcome this problem, recall that our objective is simply to find a noise sample that lies on the LR subspace; there is no need to find the exact projection of a noise sample. Therefore, an *imprecise* projection suffices to act as the noise to estimate the gradient. One efficient projection we found is the gradient of Eq. (16), written as

$$u^* \triangleq \nabla_u \|\text{scale}(x + u) - (\text{scale}(x) + u')\|_2. \quad (17)$$

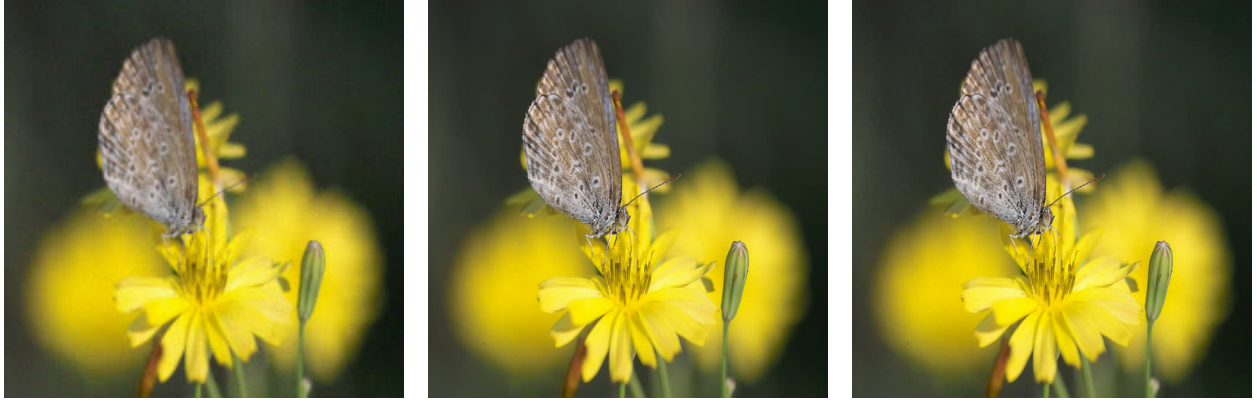
The resulting u^* is a noise sample, in the HR space, that lies on the LR subspace. Afterward, we follow the same procedure as vanilla black-box attacks, which take a set of the noise samples u^* to estimate the gradient. The gradient is the direction over which the attack searches for a new x' near the decision boundary.

6.3 Attack Median Filtering

We have shown how to incorporate the knowledge of scaling by sampling HR noise that lies on the LR subspace, as defined in Eq. (17). However, applying this technique to incorporate median filtering is prohibitive, as the median filtering function is not smooth.

We illustrate the non-smoothness problem in the context of how black-box attacks conduct line search with a direction estimated from noise samples in Eq. (17). Consider a simple example $x = [1, 3, 2]$, which results in a noise sample $u^* = [0, 0, 1]$ that leads to a similar direction $g = u^*$. This is because all non-median directions are zero. In this case, the line search procedure simply tries $\{x + g, x + 2g, \dots\}$ until reaching the decision boundary. This procedure will only increase the perturbation without changing the median value after $x + 2g$, leading to suboptimal results.

We conjecture that the root cause of this problem is the non-smoothness introduced by the median filtering. This observation is similar to that made by Chen et al. in the original black-box attack [13]. They observed that the attack does not converge when there is non-smoothness near the decision boundary. The non-smoothness of the median filtering introduces two problems. First, the attack would converge slower than before, as one might need significant perturbations to change the median output. Second, the attack could incur unnecessary perturbations, as in the example above.



(a) HopSkipJump ($\ell_2 = 5.89$)

(b) Scale-Adv ($\ell_2 = 2.03$)

(c) Scale-Adv median ($\ell_2 = 2.36$)

Figure 6: Adversarial examples from (a) HopSkipJump attack, (b) Scale-Adv attack, and (c) Scale-Adv attack under median filtering defense. The query budget is set to 5K. The original shape is 224×224 for (a), and 672×672 for (b) and (c). This shows that Scale-Adv can produce less perturbation than HopSkipJump attack even under the median filtering defense.

To mitigate this problem, we approximate the median function by “trimmed and weighted average” when computing the gradient. Specifically, for any input sequence $x \in [0, 1]^n$, we define the smoothed median function as

$$\text{smooth-median}(x) \triangleq \frac{\sum_{i=1}^n x_i \cdot \omega_i}{\sum_{i=1}^n \omega_i}, \quad (18)$$

where $\omega \in \mathbb{R}^n$ is the weighting vector.

We expect a useful weighting vector to have two properties. First, it proportionally extends the gradient to non-median values. Second, it limits the number of changed values to mitigate the perturbation. We satisfy the above two properties through quantile bounding and incorporating the absolute deviation to median. Thus, we define the weight as

$$\omega_i \triangleq (1 - |x_i - \text{median}(x)|) \cdot \mathbb{1}\{x_{(a)} \leq x_i \leq x_{(b)}\}, \quad (19)$$

where $x_{(a)}, x_{(b)}$ are the a -th and b -th quantile of scalar values in x . We empirically set (a, b) to $(0.2, 0.8)$. An empirical evaluation of this parameter can be found in Appendix B. Intuitively, values that are more deviated from the median are assigned smaller gradients. Also, the total number of changed values is limited if all values are close to the median.

Now, we have defined a median function that is useful for the black-box attack. It allows us to incorporate the knowledge of median-defended scaling using the same technique as we have described in Sec. 6.2. In particular, we invoke Eq. (17) with the original scaling function replaced by the median-defended scaling ($\text{scale} \circ \text{median}$). We do not apply this approximation when computing $\text{scale}(x)$, because this point should be precise. We note that, however, the above integration may not be optimal; we suggest future work to study more sophisticated integration.

7 Evaluation

In this section, we describe the evaluation of Scale-Adv, which targets the whole ML system in an end-to-end manner. Our evaluation is designed to answer the following questions.

Q1: How robust are add-on scaling defenses when targeting the whole ML system pipeline in a black-box setting?

We demonstrate that Scale-Adv evades four out of five scaling defenses by targeting the whole ML system under the hard-label black-box setting. These defenses include the median filtering [2] and all three detection defenses by Kim et al. [3].

Q2: Does Scale-Adv improve black-box attacks by exploiting scaling algorithms, even under scaling defenses?

Yes, Scale-Adv improves the performance of hard-label black-box attacks such as HopSkipJump by a large margin. For the same query budget, Scale-Adv can generate adversarial examples with less perturbation than the vanilla black-box attack.

Q3: Does Scale-Adv improve transfer-based black-box attacks by leveraging the weakness in scaling algorithms?

Yes, Scale-Adv produces stronger adversarial examples than vanilla C&W attack with the same perturbation budget. We demonstrate that Scale-Adv generates adversarial examples that transfer to an online commercial image classification API better than a vanilla white-box attack.

Q4: Does Scale-Adv improve white-box attacks by targeting the whole ML system pipeline? In this setting, how robust are the existing add-on scaling defenses?

Scale-Adv induces a higher drop in the classification accuracy than vanilla PGD attack with the same perturbation budget. Further, we verify that the randomized filtering defense and robust scaling algorithms are resistant to our attack in the white-box setting.

7.1 Evaluation Setup

7.1.1 Dataset and Model

We conduct all experiments on the ImageNet dataset [6] with pretrained ResNet-50 network [14]. This network accepts input images of size 224×224 .

We construct our test images with two scaling ratios. We randomly choose 251 and 252 images of the scaling ratio within the range $[3, 4)$ and $[4, 10)$. We then downscale these images to 672×672 and 896×896 , which constitute the set of clean source images with scaling ratios 3 and 4.

We base our evaluations on two models. In the black-box setting, we use the pre-trained model from PyTorch [22], which achieves 76.15% accuracy. In the white-box setting, we use an adversarially trained model [23], which achieves 57.90% accuracy on benign inputs and 35.09% accuracy under a 100-step PGD attack with ℓ_2 -norm budget 3.

7.1.2 Attack and Setup

We implement the Scale-Adv attack³ with all integrations in PyTorch [22] and ART [24].

For the HopSkipJump [13] attack, we set the query budget to $\{1000, 2000, \dots, 25000\}$. To stay consistent with previous work studying hard-label black-box attacks, we test on 100 randomly sampled images with a scaling ratio of 3.

For the C&W [4] attack, we set the binary search step to 20 with a maximum of 100 iterations. We set the confidence κ to $\{0, 1, \dots, 10\}$. We test on all images with a scaling ratio of 3.

³We plan to release the source code for Scale-Adv.

For the PGD [5] attack, we set the number of steps to 100 with ℓ_2 -norm budget $\epsilon = \{1, 2, \dots, 20\}$ and step size $0.1 \times \epsilon$. We test on all images with scaling ratios 3 and 4.

For the transfer-based attack, we demonstrate the transferability to Tencent Cloud’s “Image Analysis” API. It accepts a variety of images and returns Top-5 labels (with probability scores) that best describe the image. We define the ground truth label as the benign input’s Top-1 label; we only consider benign inputs whose Top-1 score is at least 50%. A successful attack should decrease the true label’s score to below 10%. From Xiao et al. [1], this API uses OpenCV’s linear scaling without any defenses. We employ the robust model that we used in white-box settings as the surrogate model; attacks on a non-robust model cannot transfer to this API.

We demonstrate our attack on OpenCV’s linear scaling algorithm. We conduct all experiments on an RTX 2080 Ti GPU with 11 GB memory.

7.1.3 Metrics

We use scaled ℓ_2 -norm distance to quantify the perturbation’s size. It normalizes the common ℓ_2 -norm distance by the scaling ratio against standard input size 224×224 . This metric allows for comparing perturbations between different dimensions. When referring to the perturbation of adversarial examples, we always compute such perturbation against their benign images in the same dimension. For a set of test images, we report the median ℓ_2 -norm distance between perturbed and original samples over this set of images. This metric is commonly used by previous work studying black-box attacks [13].

We also report the success rate at various ℓ_2 -norm distance thresholds, given a particular budget [13]. For instance, under the query budget q (or confidence requirement κ), the success rate can be defined as the portion of successful adversarial examples (over a set of images) whose ℓ_2 -norm perturbation is less than a threshold. This metric is closely related to the attack’s performance under the ℓ_2 -norm constraint.

Another metric we report is the Top-1 accuracy for benign and adversarial inputs. To handle input images of different shapes, all images larger than the network’s input size are filtered (if a defense is applied) and downscaled (with the respective scaling algorithm) before feeding to the network. For randomized filtering defense, we repeat such procedure 100 times and report as a correct prediction only if at least 90% of them are correct.

7.2 Evaluation of Defenses against Scaling Attacks

We start the evaluation by evaluating the defenses (against scaling attacks) using black-box Scale-Adv, which integrates the HopSkipJump attack as described in Sec. 6. The objective of this evaluation is to evaluate the prevention and detection defenses when their clean-image assumption does not hold. Recall that scaling defenses with this assumption are effective for two reasons: (1) the prevention defense can force the attack to produce significant distortions; (2) the detection defenses can distinguish between benign and attack images.

Our hypothesis is when adversaries target the ML system in an end-to-end manner, they can bypass the clean-image assumption; they can generate attack images that evade the scaling defenses and induce misclassifications. We have conducted this experiment to verify this hypothesis in two stages. First, we use Scale-Adv to generate attack images on both undefended and median-defended scaling algorithms. Second, we run detection defenses on the above attack images. We set the query budget to 5K in this evaluation.

Fig. 7 shows the distribution of distortions as measured by the unscaling defense. Recall that the unscaling defense measures the distortion between the original input image and the upscaled image after applying the downscaling. The distribution of the distortion is very similar between benign and attack images.

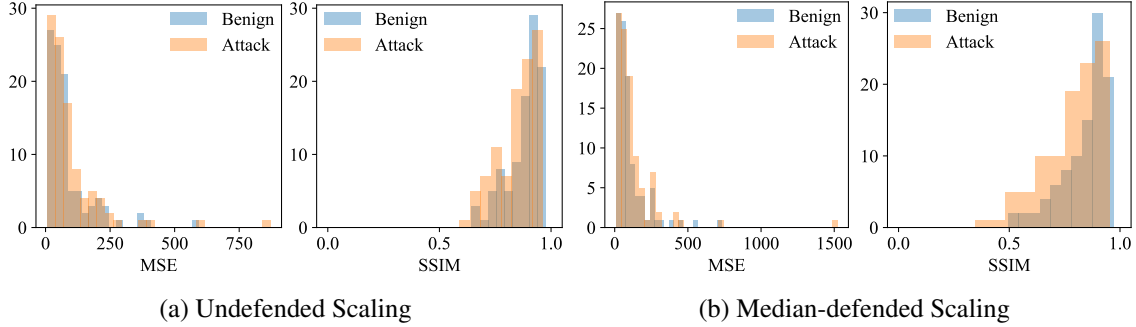


Figure 7: The histogram of distortions as measured by the unscaling defense. There does not exist a reasonable threshold to distinguish benign and attack images from Scale-Adv (5K queries) even under the median-defended scaling algorithm.

It is clear from the plots that there does not exist a reasonable threshold that allows for acceptable false acceptance and rejection rates; the Scale-Adv attack evades such threshold-based detectors. The same observations hold for the undefended and median-defended scaling. We do not report the results from the minimum-filtering defense as they show similar observations.

Fig. 8 shows the centered spectrum for example benign and attack images. This defense detects the scaling attack by identifying more than one “centered spectrum point” in the spectrum image [3] (Fig. 8b). However, the attack images from Scale-Adv do not exhibit such artifacts, as evident from the example images. Since the authors of this defense did not release its detailed implementation and settings, we were not able to fully replicate the defense’s operation. Finally, even if a learning-based model is implemented for detection defenses (instead of a threshold-based mechanism), we have described a methodology in Sec. 5.4 to incorporate such defenses in the Scale-Adv attack framework. As detection defenses are ineffective in the worst case, we do not evaluate these defenses in the following experiments.

This experiment also highlights how the median filtering defense fails to provide protection against Scale-Adv in the black-box setting. Even in the presence of median-defended scaling, Scale-Adv was able to generate adversarial examples that evade the classifier without significant distortions, as evident in Fig. 7. A more systematic analysis of the median defense is presented in the following subsection.

7.3 Hard-label Black-box Attacks

In this experiment, we evaluate how Scale-Adv improves black-box attacks, even in the presence of a defended scaling algorithm. These improvements manifest as generating less perturbed adversarial examples with the same query budget; they motivate the use of Scale-Adv to target the whole ML pipeline instead of a standalone model. Further, we show how Scale-Adv evades the median filtering defense in the black-box setting.

We integrate Scale-Adv with the HopSkipJump attack and set the query budget q to $\{1000, 2000, \dots, 25000\}$. We conduct the experiment in two steps. For each query budget q , we first use HopSkipJump to generate a set of LR adversarial examples $\mathcal{L}(q)$, and then use Scale-Adv to generate a set of HR adversarial examples $\mathcal{H}(q)$. Our objective is to show that examples in $\mathcal{H}(q)$ have less perturbation than those in $\mathcal{L}(q)$. Note that we do not use vanilla HopSkipJump attack to generate HR adversarial examples. As we have discussed in Sec. 6, it cannot leverage the weakness of scaling algorithms to target the entire ML system pipeline.

Fig. 9a shows the median perturbation of the attacks with given query budgets. For undefended scaling,

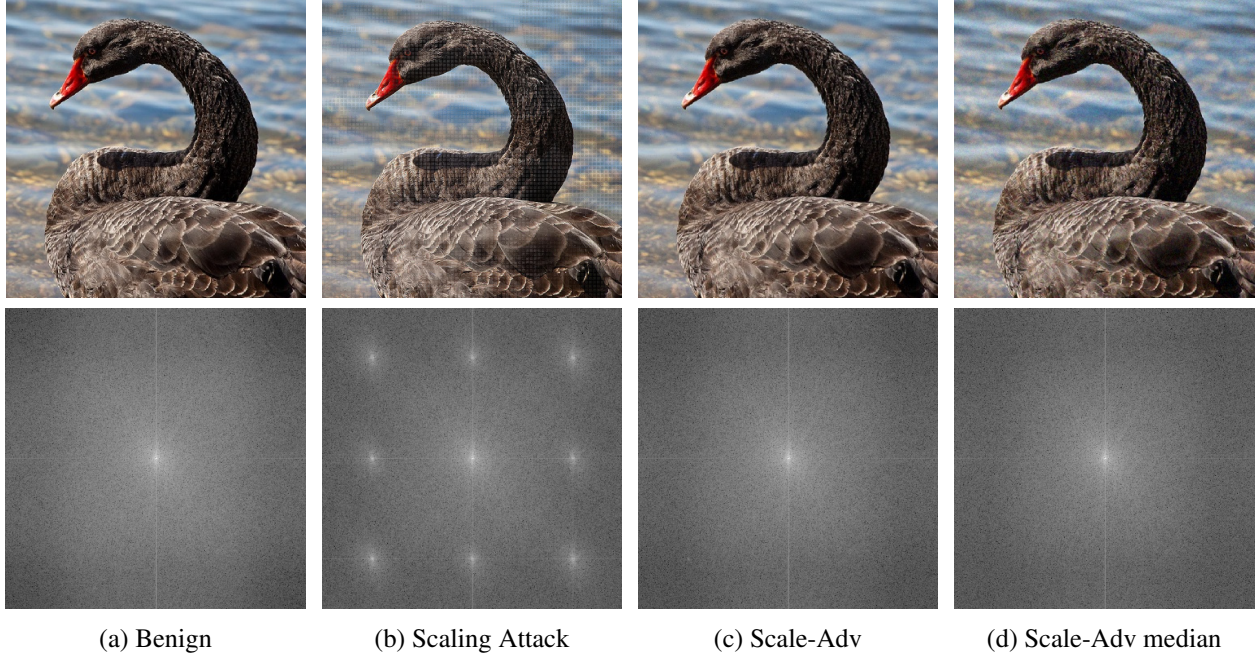


Figure 8: Examples of centered spectrum. Scaling attack shows multiple “centered spectrum points” as defined in [3]. Scale-Adv with 5K hard-label queries only shows one such point.

Scale-Adv can reduce the perturbation by a large margin. The generated adversarial examples still evade a detection defense. For median-defended scaling, Scale-Adv can converge faster to a better solution (the y-axis in the plot is in log scale).

Fig. 9b shows the success rate of the two attacks with given perturbation budgets. For undefended scaling, Scale-Adv outperforms HopSkipJump by a large margin. Similarly, for median-defended scaling, Scale-Adv outperforms HopSkipJump for the same query budget. It is clear from the plot how the dashed lines of Scale-Adv are above the dotted lines of HopSkipJump, even with 5K fewer query budgets.

7.4 Transfer-based Black-box Attacks

Another venue for a black-box attack is to leverage the well-known transferability property of adversarial examples. In this scenario, we use the Scale-Adv integration with a white-box attack to target a surrogate model. We then evaluate the success of Scale-Adv in generating adversarial examples that transfer to the Tencent Cloud’s online API. We also compare that to the success of the vanilla C&W in transferring to the online API with the same perturbation budget.

We integrate Scale-Adv with the C&W attack and set its confidence κ to $\{0, 1, \dots, 10\}$. We construct the transfer-based attack in two steps. First, we apply the attack to a surrogate model to generate adversarial examples. Second, we evaluate such examples with the online API. We perform this procedure for the C&W and Scale-Adv attacks, which result in the set of LR and HR examples $\mathcal{L}(\kappa)$ and $\mathcal{H}(\kappa)$, respectively. Our objective is to show that examples in $\mathcal{H}(\kappa)$ have less perturbation (and higher transferability) than those in $\mathcal{L}(\kappa)$.

We start by evaluating the improvement to the C&W attack in the white-box setting. In Fig.10, we clearly observe that Scale-Adv can improve the vanilla C&W attack by a large margin; for the same confidence,

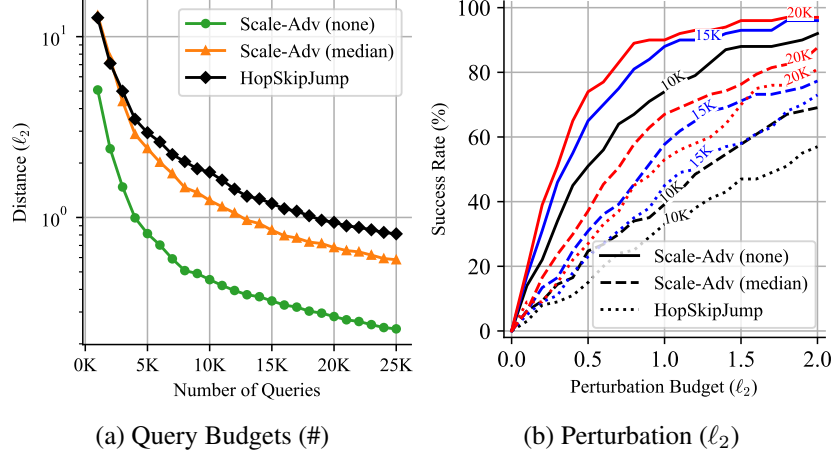


Figure 9: Compare the performance of our Scale-Adv attack and the vanilla HopSkipJump attack under different requirements.

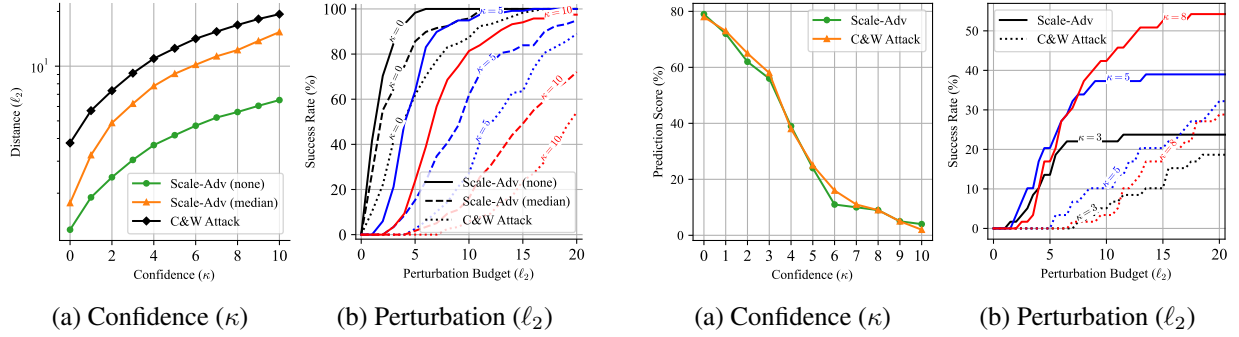


Figure 10: Compare the performance of our Scale-Adv attack and the vanilla C&W attack under different requirements.

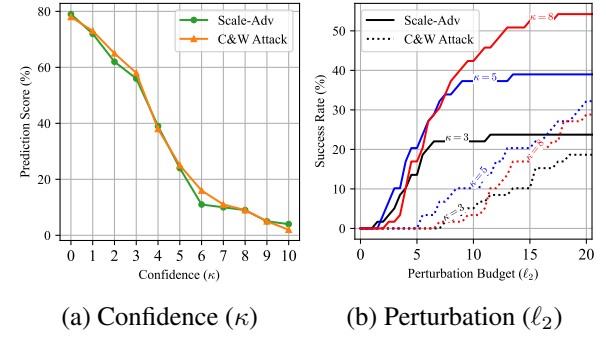


Figure 11: Compare the transferability of our Scale-Adv attack and the vanilla C&W attack on Tencent Cloud API.

it requires much less perturbation (Fig. 10a). Scale-Adv has a much higher success rate than the vanilla C&W attack for a given ℓ_2 -norm perturbation requirement (Fig. 10b). This result verifies the effectiveness of Scale-Adv over powerful white-box attacks such as C&W in a setting where the model is part of a larger system that contains the upstream scaling algorithms.

We then evaluate the above adversarial examples with the Tencent Cloud’s online API. We only consider undefended scaling as this API has not implemented any defenses against the scaling attack. In Fig. 11, we clearly observe that Scale-Adv can improve transfer-based attacks by a large margin. While it is unsurprising that Scale-Adv obtains similar transferability as C&W if given the same confidence (Fig. 11a), Scale-Adv has a significantly higher success rate than the vanilla C&W attack for a given ℓ_2 -norm perturbation requirement (Fig. 11b). This result clearly verifies the improvement of Scale-Adv to transfer-based attacks by exploiting the scaling algorithm.

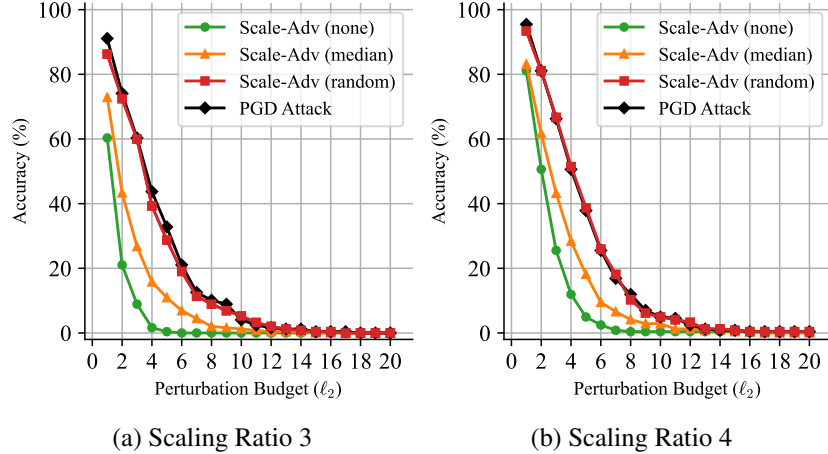


Figure 12: Compare the performance of our Scale-Adv and the vanilla PGD attack under different scaling defenses.

7.5 White-box Attacks

Finally, we evaluate the robustness of existing scaling defenses against a white-box attacker with full access to the model parameters. This evaluation allows us to assess the worst-case performance of scaling defenses. In order to evaluate the performance under perturbation budgets, we integrate Scale-Adv with the PGD attack, which directly upper bounds the perturbation. As before, we generate two sets of adversarial examples, $\mathcal{L}(\epsilon)$ and $\mathcal{H}(\epsilon)$, using PGD and Scale-Adv, respectively.

For completeness, we evaluate all prevention defenses on two scaling ratios. Fig. 12 shows the model’s accuracy under different attacks and perturbation budgets. It is evident from the figure that Scale-Adv can improve the vanilla PGD attack by a large margin for undefended and median-defended scaling. However, such improvement disappears on random-defended scaling algorithms. This result verifies our arguments about the median filtering being non-robust while the randomized filtering defense is robust.

In summary, Scale-Adv has shown that most of the add-on defenses (i.e., prevention and detection defenses) cannot handle adversarial perturbations because of their clean-image assumption. However, randomized filtering-based defenses and scaling algorithms that adopt uniform kernels or dynamic kernel widths (evaluated in Appendix C) are robust even when the adversary attempts to jointly attack the downstream model. These approaches uniformly consider the pixel in a window, forcing the adversary to perturb all such pixels. Going forward, we recommend that existing and future ML systems migrate to scaling algorithms that are robust by design.

8 Discussions

Below, we discuss the limitations of Scale-Adv and possible future directions to mitigate similar threats in an ML system.

8.1 Limitations

As the proposed Scale-Adv attack combines scaling and ML attacks, it also inherits a few limitations from both sides. First, our attack produces images that downscale to an adversarial example; thus, an anomaly

detector could potentially detect it. However, we note that our attack framework could also incorporate adaptive attacks against such defenses.

Second, our attack evades most scaling defenses by leveraging the small magnitude of adversarial perturbations. We note that such property may not hold in targeted black-box attacks or white-box C&W attacks with a high confidence value.

Finally, we note that our attack relies on the vulnerability of image scaling. This attack is blocked if ML systems start using robust scaling algorithms. We hope our results motivate their use instead of weaker add-on defenses.

8.2 Future Work

8.2.1 Defenses against Black-box Attacks

In this paper, we find that integrating hard-label attacks with the median filtering defense is challenging (refer to Sec. 6.3). Although such defense is designed to mitigate the scaling attack, there exist similar defenses against adversarial examples [25]. While attacking preprocessing defenses has been well studied in the white-box setting [26], it is unclear how to circumvent such defenses efficiently in the black-box setting. They effectively break the smoothness assumption of black-box attacks. We suggest future work to explore black-box attacks and defenses based on non-smooth preprocessing.

8.2.2 ML Defense Evasion

Our empirical evaluation shows that an attacker can leverage the scaling algorithm to improve white-box attacks even against adversarially trained models. This observation directly poses a threat to the downstream ML defenses, including certified defenses [27]. For example, consider an ML defense that certifies adversarial robustness within an ℓ_2 -norm ball of radius ϵ . In this case, the proposed Scale-Adv attack could produce an HR adversarial example with (scaled) ℓ_2 -norm perturbation less than ϵ , but downscales to an LR adversarial example with perturbation larger than ϵ , thereby evading the ϵ -certification. We suggest future work to explore threats to the ML defense from other modalities.

9 Related Work

This paper proposes a new attack framework that jointly targets the scaling algorithm and ML classifier. Therefore, we discuss related work in both areas.

9.1 Image-Scaling Attacks

The image-scaling attack was first proposed by Xiao et al. [1] and then improved by Quiring et al. [2] and Chen et al. [16]. Nevertheless, all variants of this attack have been shown ineffective under several defenses, including prevention defenses [2] and detection defenses [3]. Such defenses have empirically mitigated the threat from image-scaling attacks.

However, the above attacks and defenses are tailored to the image-scaling stage. In contrast, this paper looks at this problem from the perspective of the entire ML system, which includes both the scaling and classification stages. Our theoretical and empirical analysis shows that most defenses are not designed to handle adversarial perturbations.

As a result, this paper demonstrates that the image-scaling stage is still vulnerable if viewing together with the classification stage. We empirically observe that both black-box and white-box ML attacks are able to leverage this vulnerability to improve their performance by a large margin. This observation poses new threats to ML systems that include scaling.

9.2 Adversarial Machine Learning

This paper demonstrates that Scale-Adv can improve the performance of black-box attacks such as HopSkipJump [13] by leveraging the benefits of scaling attacks. In particular, it modifies the typical noise sampling step in black-box attacks, thereby sampling HR noise that lies on an LR subspace.

Some recent works have used a similar but different technique to improve black-box attacks, such as QEBA [28] and Nonlinear-QEBA [29]. These methods leverage dimension-reduction techniques to find a low-dimensional (LD) space and conduct the gradient estimation. However, these methods take place in the LR input space; they do not have knowledge of the upstream scaling algorithm. In contrast, we exploit the HR space. Further, they estimate the gradient in LD space and then project it back to LR space. This approach cannot invert the median projection that we exploit, as it involves solving a complicated optimization problem for *every* noise sample. To mitigate this problem, we propose an imperfect projection using its gradient. Since we exploit different spaces to improve the attack, our improvement is orthogonal to their methods. It is possible to combine the benefits of both attacks.

Further, we note that the proposed attack framework can integrate other ML attacks as well. For example, transfer-based attacks on face recognition systems [30–33] can leverage the benefits of our attack to produce stronger and less perturbed adversarial examples. We notice that the attack from Cherepanova et al. [33] has implicitly exploited the scaling vulnerability; our paper provides a deeper understanding of this mechanism.

10 Conclusion

This paper presents the Scale-Adv attack framework, which leverages the vulnerability of both scaling algorithms and ML classifiers for vision tasks. By targeting the entire ML system, an attacker can improve the performance of ML attacks while evading most existing defenses against the scaling attack. We studied cutting-edge attacks in both black-box and white-box settings, such as HopSkipJump, C&W, and PGD. Our results exhibit that an attacker can produce stronger adversarial examples with less perturbation and lower query budgets if targeting the entire ML system. The purpose of this work is to raise the concern of threats that jointly exploit different components in the ML system. We believe that further work is necessary to identify and mitigate other threats that jointly target different stages in the ML system.

References

- [1] Q. Xiao, Y. Chen, C. Shen, Y. Chen, and K. Li, “Seeing is not believing: Camouflage attacks on image scaling algorithms,” in *28th USENIX Security Symposium, USENIX Security 2019, Santa Clara, CA, USA, August 14-16, 2019*, N. Heninger and P. Traynor, Eds. USENIX Association, 2019, pp. 443–460. [Online]. Available: <https://www.usenix.org/conference/usenixsecurity19/presentation/xiao>
- [2] E. Quiring, D. Klein, D. Arp, M. Johns, and K. Rieck, “Adversarial preprocessing: Understanding and preventing image-scaling attacks in machine learning,” in *29th USENIX Security Symposium, USENIX Security 2020, August 12-14, 2020*, 2020, pp. 1363–1380. [Online]. Available: <https://www.usenix.org/conference/usenixsecurity20/presentation/quiring>
- [3] B. Kim, A. Abuadbbba, Y. Gao, Y. Zheng, M. E. Ahmed, H. Kim, and S. Nepal, “Decamouflage: A framework to detect image-scaling attacks on convolutional neural networks,” *CoRR*, vol. abs/2010.03735, 2020. [Online]. Available: <https://arxiv.org/abs/2010.03735>
- [4] N. Carlini and D. A. Wagner, “Towards evaluating the robustness of neural networks,” in *2017 IEEE Symposium on Security and Privacy, SP 2017, San Jose, CA, USA, May 22-26, 2017*. IEEE Computer Society, 2017, pp. 39–57. [Online]. Available: <https://doi.org/10.1109/SP.2017.49>
- [5] A. Madry, A. Makelov, L. Schmidt, D. Tsipras, and A. Vladu, “Towards deep learning models resistant to adversarial attacks,” in *6th International Conference on Learning Representations, ICLR 2018, Vancouver, BC, Canada, April 30 - May 3, 2018, Conference Track Proceedings*. OpenReview.net, 2018. [Online]. Available: <https://openreview.net/forum?id=rJzIBfZAb>
- [6] O. Russakovsky, J. Deng, H. Su, J. Krause, S. Satheesh, S. Ma, Z. Huang, A. Karpathy, A. Khosla, M. S. Bernstein, A. C. Berg, and F. Li, “Imagenet large scale visual recognition challenge,” *Int. J. Comput. Vis.*, vol. 115, no. 3, pp. 211–252, 2015. [Online]. Available: <https://doi.org/10.1007/s11263-015-0816-y>
- [7] C. Szegedy, V. Vanhoucke, S. Ioffe, J. Shlens, and Z. Wojna, “Rethinking the inception architecture for computer vision,” in *2016 IEEE Conference on Computer Vision and Pattern Recognition, CVPR 2016, Las Vegas, NV, USA, June 27-30, 2016*. IEEE Computer Society, 2016, pp. 2818–2826. [Online]. Available: <https://doi.org/10.1109/CVPR.2016.308>
- [8] C. Szegedy, S. Ioffe, V. Vanhoucke, and A. A. Alemi, “Inception-v4, inception-resnet and the impact of residual connections on learning,” in *Proceedings of the Thirty-First AAAI Conference on Artificial Intelligence, February 4-9, 2017, San Francisco, California, USA*, S. P. Singh and S. Markovitch, Eds. AAAI Press, 2017, pp. 4278–4284. [Online]. Available: <http://aaai.org/ocs/index.php/AAAI/AAAI17/paper/view/14806>
- [9] J. Redmon, S. K. Divvala, R. B. Girshick, and A. Farhadi, “You only look once: Unified, real-time object detection,” in *2016 IEEE Conference on Computer Vision and Pattern Recognition, CVPR 2016, Las Vegas, NV, USA, June 27-30, 2016*. IEEE Computer Society, 2016, pp. 779–788. [Online]. Available: <https://doi.org/10.1109/CVPR.2016.91>
- [10] C. Szegedy, W. Zaremba, I. Sutskever, J. Bruna, D. Erhan, I. J. Goodfellow, and R. Fergus, “Intriguing properties of neural networks,” *CoRR*, vol. abs/1312.6199, 2013. [Online]. Available: <http://arxiv.org/abs/1312.6199>

- [11] B. Biggio, I. Corona, D. Maiorca, B. Nelson, N. Šrndić, P. Laskov, G. Giacinto, and F. Roli, “Evasion attacks against machine learning at test time,” in *Joint European conference on machine learning and knowledge discovery in databases*. Springer, 2013, pp. 387–402.
- [12] N. Carlini, A. Athalye, N. Papernot, W. Brendel, J. Rauber, D. Tsipras, I. Goodfellow, A. Madry, and A. Kurakin, “On evaluating adversarial robustness,” 2019.
- [13] J. Chen, M. I. Jordan, and M. J. Wainwright, “Hopskipjumpattack: A query-efficient decision-based attack,” in *2020 IEEE Symposium on Security and Privacy, SP 2020, San Francisco, CA, USA, May 18-21, 2020*. IEEE, 2020, pp. 1277–1294. [Online]. Available: <https://doi.org/10.1109/SP40000.2020.00045>
- [14] K. He, X. Zhang, S. Ren, and J. Sun, “Deep residual learning for image recognition,” in *2016 IEEE Conference on Computer Vision and Pattern Recognition, CVPR 2016, Las Vegas, NV, USA, June 27-30, 2016*. IEEE Computer Society, 2016, pp. 770–778. [Online]. Available: <https://doi.org/10.1109/CVPR.2016.90>
- [15] V. Dumoulin and F. Visin, “A guide to convolution arithmetic for deep learning,” *CoRR*, vol. abs/1603.07285, pp. 6–8, 2016. [Online]. Available: <http://arxiv.org/abs/1603.07285>
- [16] Y. Chen, C. Shen, C. Wang, Q. Xiao, K. Li, and Y. Chen, “Scaling camouflage: Content disguising attack against computer vision applications,” *IEEE Transactions on Dependable and Secure Computing*, 2020.
- [17] V. Dumoulin and F. Visin, “A guide to convolution arithmetic for deep learning,” *CoRR*, vol. abs/1603.07285, pp. 6–8, 2016. [Online]. Available: <http://arxiv.org/abs/1603.07285>
- [18] A. Ben-Israel and T. N. Greville, *Generalized inverses: theory and applications*. Springer Science & Business Media, 2003, vol. 15.
- [19] A. Athalye, L. Engstrom, A. Ilyas, and K. Kwok, “Synthesizing robust adversarial examples,” in *Proceedings of the 35th International Conference on Machine Learning, ICML 2018, Stockholmsmässan, Stockholm, Sweden, July 10-15, 2018*, ser. Proceedings of Machine Learning Research, J. G. Dy and A. Krause, Eds., vol. 80. PMLR, 2018, pp. 284–293. [Online]. Available: <http://proceedings.mlr.press/v80/athalye18b.html>
- [20] N. Carlini and H. Farid, “Evading deepfake-image detectors with white- and black-box attacks,” in *2020 IEEE/CVF Conference on Computer Vision and Pattern Recognition, CVPR Workshops 2020, Seattle, WA, USA, June 14-19, 2020*. IEEE, 2020, pp. 2804–2813. [Online]. Available: <https://doi.org/10.1109/CVPRW50498.2020.00337>
- [21] J. Frank, T. Eisenhofer, L. Schönherr, A. Fischer, D. Kolossa, and T. Holz, “Leveraging frequency analysis for deep fake image recognition,” in *Proceedings of the 37th International Conference on Machine Learning, ICML 2020, 13-18 July 2020, Virtual Event*, ser. Proceedings of Machine Learning Research, vol. 119. PMLR, 2020, pp. 3247–3258. [Online]. Available: <http://proceedings.mlr.press/v119/frank20a.html>
- [22] A. Paszke, S. Gross, F. Massa, A. Lerer, J. Bradbury, G. Chanan, T. Killeen, Z. Lin, N. Gimelshein, L. Antiga, A. Desmaison, A. Kopf, E. Yang, Z. DeVito, M. Raison, A. Tejani,

- S. Chilamkurthy, B. Steiner, L. Fang, J. Bai, and S. Chintala, “Pytorch: An imperative style, high-performance deep learning library,” in *Advances in Neural Information Processing Systems* 32, H. Wallach, H. Larochelle, A. Beygelzimer, F. d'Alché-Buc, E. Fox, and R. Garnett, Eds. Curran Associates, Inc., 2019, pp. 8024–8035. [Online]. Available: <http://papers.neurips.cc/paper/9015-pytorch-an-imperative-style-high-performance-deep-learning-library.pdf>
- [23] L. Engstrom, A. Ilyas, H. Salman, S. Santurkar, and D. Tsipras, “Robustness (python library),” 2019. [Online]. Available: <https://github.com/MadryLab/robustness>
- [24] M.-I. Nicolae, M. Sinn, M. N. Tran, B. Buesser, A. Rawat, M. Wistuba, V. Zantedeschi, N. Baracaldo, B. Chen, H. Ludwig, I. Molloy, and B. Edwards, “Adversarial robustness toolbox v1.6.0,” *CoRR*, vol. 1807.01069, 2018. [Online]. Available: <https://arxiv.org/pdf/1807.01069>
- [25] C. Guo, M. Rana, M. Cissé, and L. van der Maaten, “Countering adversarial images using input transformations,” in *6th International Conference on Learning Representations, ICLR 2018, Vancouver, BC, Canada, April 30 - May 3, 2018, Conference Track Proceedings*. OpenReview.net, 2018. [Online]. Available: <https://openreview.net/forum?id=SyJ7CIWCb>
- [26] A. Athalye, N. Carlini, and D. A. Wagner, “Obfuscated gradients give a false sense of security: Circumventing defenses to adversarial examples,” in *Proceedings of the 35th International Conference on Machine Learning, ICML 2018, Stockholmsmässan, Stockholm, Sweden, July 10-15, 2018*, ser. Proceedings of Machine Learning Research, J. G. Dy and A. Krause, Eds., vol. 80. PMLR, 2018, pp. 274–283. [Online]. Available: <http://proceedings.mlr.press/v80/athalye18a.html>
- [27] J. M. Cohen, E. Rosenfeld, and J. Z. Kolter, “Certified adversarial robustness via randomized smoothing,” in *Proceedings of the 36th International Conference on Machine Learning, ICML 2019, 9-15 June 2019, Long Beach, California, USA*, ser. Proceedings of Machine Learning Research, K. Chaudhuri and R. Salakhutdinov, Eds., vol. 97. PMLR, 2019, pp. 1310–1320. [Online]. Available: <http://proceedings.mlr.press/v97/cohen19c.html>
- [28] H. Li, X. Xu, X. Zhang, S. Yang, and B. Li, “QEBA: query-efficient boundary-based blackbox attack,” in *2020 IEEE/CVF Conference on Computer Vision and Pattern Recognition, CVPR 2020, Seattle, WA, USA, June 13-19, 2020*. IEEE, 2020, pp. 1218–1227. [Online]. Available: <https://doi.org/10.1109/CVPR42600.2020.00130>
- [29] H. Li, L. Li, X. Xu, X. Zhang, S. Yang, and B. Li, “Nonlinear projection based gradient estimation for query efficient blackbox attacks,” *CoRR*, vol. abs/2102.13184, 2021. [Online]. Available: <https://arxiv.org/abs/2102.13184>
- [30] V. Chandrasekaran, C. Gao, B. Tang, K. Fawaz, S. Jha, and S. Banerjee, “Face-off: Adversarial face obfuscation,” *Proceedings on Privacy Enhancing Technologies*, vol. 2021, 2021.
- [31] I. Evtimov, P. Sturmfels, and T. Kohno, “Foggsight: A scheme for facial lookup privacy,” *CoRR*, vol. abs/2012.08588, 2020. [Online]. Available: <https://arxiv.org/abs/2012.08588>
- [32] S. Shan, E. Wenger, J. Zhang, H. Li, H. Zheng, and B. Y. Zhao, “Fawkes: Protecting privacy against unauthorized deep learning models,” in *29th USENIX Security Symposium, USENIX Security 2020, August 12-14, 2020*, S. Capkun and F. Roesner, Eds. USENIX Association, 2020, pp. 1589–1604. [Online]. Available: <https://www.usenix.org/conference/usenixsecurity20/presentation/shan>

- [33] V. Cherepanova, M. Goldblum, H. Foley, S. Duan, J. P. Dickerson, G. Taylor, and T. Goldstein, “Lowkey: Leveraging adversarial attacks to protect social media users from facial recognition,” *CoRR*, vol. abs/2101.07922, 2021. [Online]. Available: <https://arxiv.org/abs/2101.07922>
- [34] *6th International Conference on Learning Representations, ICLR 2018, Vancouver, BC, Canada, April 30 - May 3, 2018, Conference Track Proceedings*. OpenReview.net, 2018. [Online]. Available: <https://openreview.net/group?id=ICLR.cc/2018/Conference>
- [35] J. G. Dy and A. Krause, Eds., *Proceedings of the 35th International Conference on Machine Learning, ICML 2018, Stockholmsmässan, Stockholm, Sweden, July 10-15, 2018*, ser. Proceedings of Machine Learning Research, vol. 80. PMLR, 2018. [Online]. Available: <http://proceedings.mlr.press/v80/>
- [36] *2016 IEEE Conference on Computer Vision and Pattern Recognition, CVPR 2016, Las Vegas, NV, USA, June 27-30, 2016*. IEEE Computer Society, 2016. [Online]. Available: <https://ieeexplore.ieee.org/xpl/conhome/7776647/proceeding>

A Analysis of the Randomized Filtering Defense

In the following arguments, we show that the randomized filtering defense indeed meets the robustness requirement.

Without loss of generality, we study randomized filtering over a 3×3 window w in the source image S and an arbitrary convolution kernel k . We also pad the input properly so the window w is always surrounded by other pixels. Since both the scaling and filtering functions can be written as a convolution, we restate the defended scaling $D = (\text{scale} \circ \text{defense})(S)$ over a window w with output pixel $d_{2,2}$ as

$$\begin{aligned} d_{2,2} &= w \star f_{\text{rnd}} \star k \\ &= \begin{bmatrix} w_{1,1} & w_{1,2} & w_{1,3} \\ w_{2,1} & w_{2,2} & w_{2,3} \\ w_{3,1} & w_{3,2} & w_{3,3} \end{bmatrix} \star f_{\text{rnd}} \star \begin{bmatrix} k_{1,1} & k_{1,2} & k_{1,3} \\ k_{2,1} & k_{2,2} & k_{2,3} \\ k_{3,1} & k_{3,2} & k_{3,3} \end{bmatrix}, \end{aligned}$$

where the randomized filter f_{rnd} randomly picks a pixel from the 3×3 input window w with probability $1/9$.

We study the central pixel $w_{2,2}$ and its weight $w'_{2,2}$ during this defended scaling. First, the randomized filtering slides a 3×3 window around each pixel $w_{i,j}$ and randomly changes its value to $w_{2,2}$ with a probability $\Pr[w_{i,j} \leftarrow w_{2,2}] = 1/9$. Second, the scaling algorithm gives the weight $k_{i,j}$ to each pixel $w_{i,j}$. Since the pixel $w_{i,j}$ could hold the value of $w_{2,2}$, the overall weight of $w_{2,2}$ can be described as $\Pr[w'_{2,2} \leftarrow k_{i,j}] = 1/9$. Thus, we can write the expected value of the weight $w'_{2,2}$ as

$$\mathbb{E}_{f \sim \mathcal{F}}[w'_{2,2}] = \sum_{1 \leq i,j \leq 3} \frac{1}{9} \cdot k_{i,j} = \frac{1}{9}, \quad (20)$$

where \mathcal{F} is the filter space determined by f_{rnd} and we have assumed a normalized scaling kernel k . This shows that the pixel $w_{2,2}$ is given a uniform weight in expectation. Extending this result to other pixels, we have:

$$\mathbb{E}_{\text{defense} \sim \mathcal{D}}[(\text{scale} \circ \text{defense})(S)] = S \star k_{\text{area}}, \quad (21)$$

where \mathcal{D} is the space of defense functions chosen by the randomized filtering defense and k_{area} is the uniform area scaling kernel defined in Sec.2.3.3.

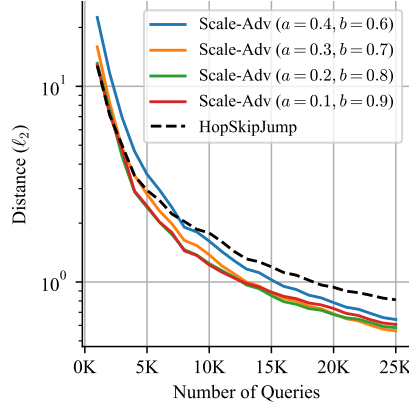


Figure 13: Compare the performance of our Scale-Adv attack under median-defended scaling and the vanilla HopSkipJump attack. We demonstrate different quantile bounds in Eq. (19).

B Approximation of Median’s Gradient

In Sec. 6.3, we approximate the median function by “trimmed and weighted average” to provide a useful gradient for black-box attacks. To this end, we introduce the weight with quantile bounding, as defined in Eq. (19). In this section, we provide empirical evaluations of different choices of the quantile position a and b .

As we can observe from Fig. 13, more constrained bounds could result in suboptimal performance, such as $(0.4, 0.6)$ and $(0.3, 0.7)$. In contrast, we observe that relaxed bounds could obtain better performance, such as $(0.2, 0.8)$ and $(0.1, 0.9)$. We finally choose $(0.2, 0.8)$ as it obtains better performance when given lower query budgets (5K) and higher budgets (25K).

C Evaluate Robust Scaling Algorithms

Recall that Quiring et al. [2] have identified a few scaling algorithms that are robust against the scaling attack (see Sec. 2.3.3). We also evaluate their robustness against the proposed Scale-Adv attack. In Fig. 14, we report the evaluation of scaling algorithms that adopt uniform kernels (CV Area) or dynamic kernel widths (PIL Linear). As evident from the plots, Scale-Adv cannot exploit these scaling algorithms to improve the vanilla PGD attack. This verifies the robustness of known-robust scaling algorithms in a setting where the attacker jointly targets the whole ML system pipeline.

D Distribution of Randomized Filtering Outputs

In this section, we provide empirical evidence to show that the distortion between source and randomized-filtered images can be approximated by the Laplacian distribution. To obtain the sampling distribution of such distortions, we sample the randomized filtering for 200 times and measure the distortion between vulnerable pixels before and after filtering.

As evident from Fig. 15, the sampling distribution of such distortions is very similar to the Laplacian distribution. This observation implies that applying a randomized filtering can be approximately viewed as adding zero-mean noise to a mean value, as we have formalized in Eq. (14).

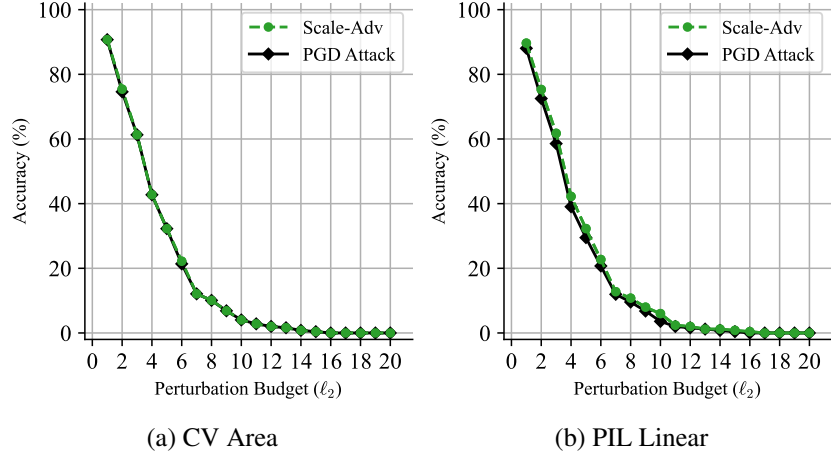


Figure 14: Compare the performance of Scale-Adv and PGD with scaling algorithms that are robust by design. This verifies the robustness of such scaling algorithms in a setting where the attacker jointly targets the whole ML system pipeline.

E More Black-box Examples (HopSkipJump)

We demonstrate more black-box adversarial examples in Fig. 16. Scale-Adv is able to produce less perturbation than the vanilla HopSkipJump attack for a given query budget. The same observation holds for median-defended scaling after 200 model queries.

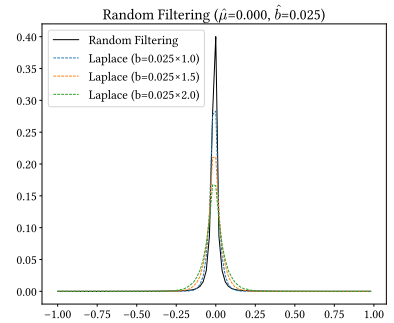
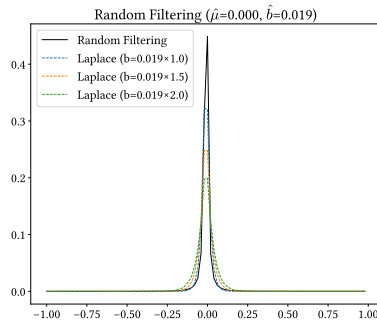
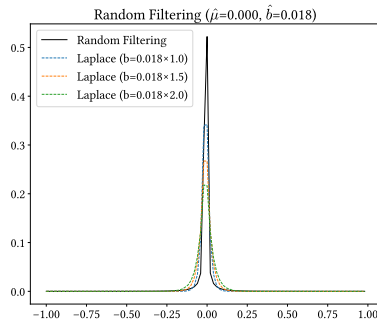
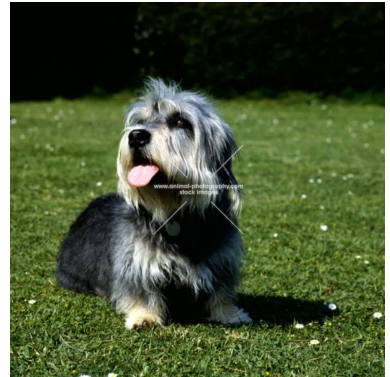
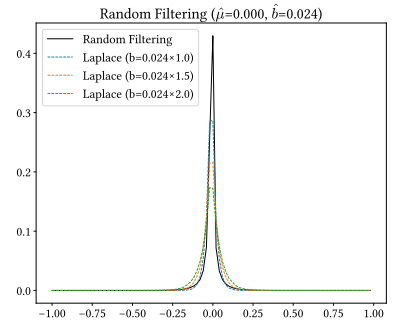
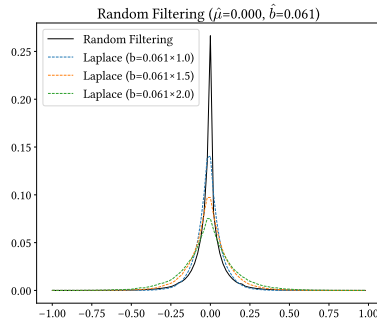
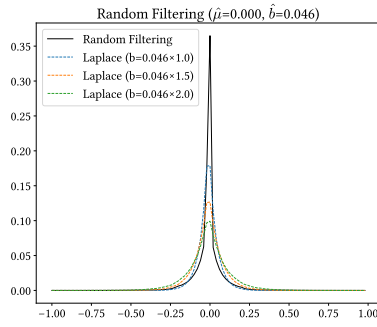


Figure 15: Sampling distribution of the perturbation from randomized filtering's output.

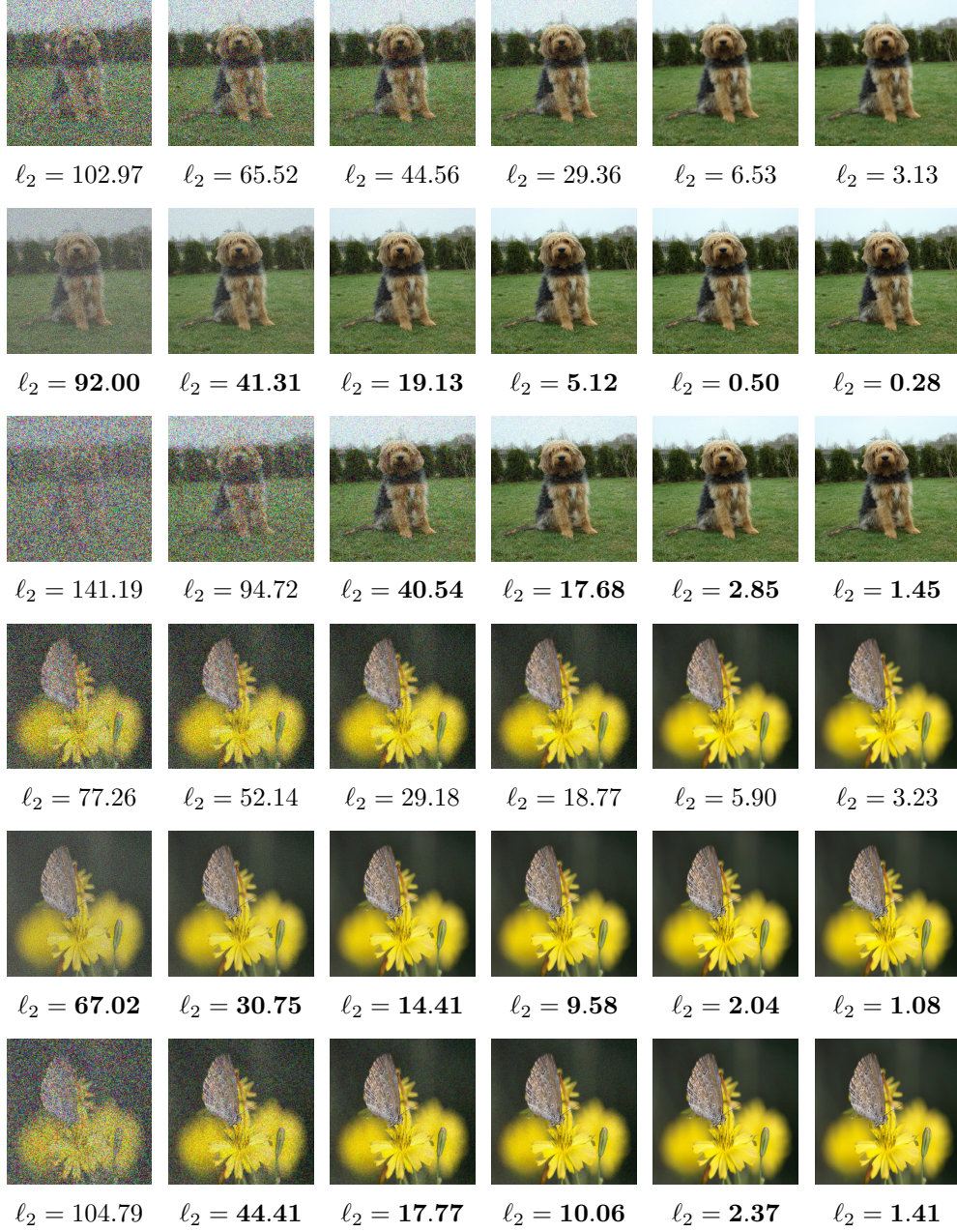


Figure 16: Adversarial examples in the black-box setting. 1st–3rd (4th–6th) rows: examples generated by HopSkipJump, Scale-Adv, and Scale-Adv under median-defended scaling. 1st–6th columns: examples at 100, 200, 500, 1K, 5K, 10K model queries. Perturbations: the scaled ℓ_2 -norm distance to the original image, numbers in bold font denote obtaining less perturbation than the vanilla HopSkipJump attack. The shape of above images by HopSkipJump and Scale-Adv is 224×224 and 672×672 , respectively.